

Article

Not peer-reviewed version

A Comparative Study of Tumor-Specificity and Neurotoxicity Between 3-Styrylchromones and Anticancer Drugs

Tomoyuki Abe , [Hiroshi Sakagami](#) ^{*} , Shigeru Amano , Shin Uota , [Kenjiro Bandow](#) , [Yoshihiro Uesawa](#) , Shiori U , Hiroki Shibata , Yuri Takemura , Yu Kimura , [Koichi Takao](#) , [Yoshiaki Sugita](#) , [Akira Sato](#) , Sei-ichi Tanuma , Hiroshi Takeshima

Posted Date: 5 June 2023

doi: 10.20944/preprints202306.0342.v1

Keywords: chromone derivatives; oral squamous cell carcinoma; tumor-specificity; keratinocyte toxicity; neurotoxicity; signaling pathway



Preprints.org is a free multidiscipline platform providing preprint service that is dedicated to making early versions of research outputs permanently available and citable. Preprints posted at Preprints.org appear in Web of Science, Crossref, Google Scholar, Scilit, Europe PMC.

Copyright: This is an open access article distributed under the Creative Commons Attribution License which permits unrestricted use, distribution, and reproduction in any medium, provided the original work is properly cited.

Article

A Comparative Study of Tumor-specificity and Neurotoxicity between 3-Styrylchromones and Anticancer Drugs

Tomoyuki Abe ^{1,†}, Hiroshi Sakagami ^{2,*†}, Shigeru Amano ², Shin Uota ², Kenjiro Bandow ³, Yoshihiro Uesawa ⁴, Shiori U ⁵, Hiroki Shibata ⁵, Yuri Takemura ⁵, Yu Kimura ⁵, Koichi Takao ⁵, Yoshiaki Sugita ⁵, Akira Sato ⁶, Sei-ichi Tanuma ² and Hiroshi Takeshima ¹

¹ Division of Geriatric Dentistry, Meikai University School of Dentistry, Saitama 350-0283, Japan; abetomoyuki0524@gmail.com (T.A.); takesima@dent.meikai.ac.jp (H.T.)

² Meikai University Research Institute of Odontology (M-RIO), 1-1 Keyakidai, Sakado 350-0283, Saitama 350-0283, Japan; shigerua@dent.meikai.ac.jp (S.A.); suota@dent.meikai.ac.jp (S.U); tanuma@dent.meikai.ac.jp (S.T.)

³ Division of Biochemistry, Meikai University School of Dentistry, Saitama, Japan; kbando@dent.meikai.ac.jp

⁴ Department of Medical Molecular Informatics, Meiji Pharmaceutical University, Tokyo 204-858, Japan; uesawa@my-pharm.ac.jp

⁵ Department of Pharmaceutical Sciences, Faculty of Pharmacy and Pharmaceutical Sciences, Josai University, Saitama 350-0295, Japan; usor516@gmail.com (S.U); mafuyu_vd@yahoo.co.jp (H.S.); chelly-egoist.shu@docomo.ne.jp (Y.T.); percbz2@gmail.com (Y.K.); ktakao@josai.ac.jp (K.T.); sugita@josai.ac.jp (Y.S.)

⁶ Department of Biochemistry and Molecular Biology, Faculty of Pharmaceutical Sciences, Tokyo University of Science, Chiba, Japan; akirasat@rs.tus.ac.jp (A.S.)

* Correspondence: sakagami@dent.meikai.ac.jp; Tel: +81-49-279-2758

† These authors contributed equally to this study.

Abstract: Background. Many anticancer drugs used in clinical practice cause adverse events such as oral mucositis, neurotoxicity, and extravascular leakage. We have reported that two 3-styrylchromone derivatives, 7-methoxy-3-[(1E)-2-phenylethenyl]-4H-1-benzopyran-4-one (compound A) and 3-[(1E)-2-(4-hydroxyphenyl)ethenyl]-7-methoxy-4H-1-benzopyran-4-one (compound B) showed the highest tumor-specificity against human oral squamous cell carcinoma (OSCC) cell lines among 291 related compounds. After confirming their superiority by comparing their tumor specificity with newly synthesized 65 derivatives, we investigated the neurotoxicity of these compounds, in comparison with 4 popular anticancer drugs. **Methods:** Tumor-specificity (TS_M , TS_E , TS_N) was evaluated as the ratio of mean CC_{50} for human normal oral mesenchymal (gingival fibroblast, pulp cell), oral epithelial cells (gingival epithelial progenitor), and neuronal cells (PC-12, SH-SY5Y, LY-PPB6, differentiated PC-12) to OSCC cells (Ca9-22, HSC-2), respectively. **Results:** Compounds A and B showed one-order of magnitude higher TS_M as compared with newly synthesized derivatives, confirming its prominent tumor-specificity. Docetaxel showed one order of magnitude higher TS_M , but two order of magnitude lower TS_E than compounds A and B. Compounds A and B showed higher TS_M , TS_E and TS_N values than doxorubicin, 5-FU and cisplatin, damaging OSCC cells at concentrations that do not affect the viability of normal epithelial and neuronal cells. QSAR prediction based on the Tox21 database suggested that compounds A and B may inhibit the signaling pathway of estrogen-related receptors.

Keywords: chromone derivatives; oral squamous cell carcinoma; tumor-specificity; keratinocyte toxicity; neurotoxicity; signaling pathway

1. Introduction

Many anticancer drugs have been reported to cause side effects such as oral mucositis, neurotoxicity, and extravasation (leak of intravenously injected drugs and fluids out of the blood vessels) in clinical practice [1-9]. Oral mucositis not only reduces the patient's quality of life due to

accompanying pain, lowers the oral intake and dehydration, and can trigger systemic bacterial infection and invasion. Reduced administration doses of chemotherapeutic drugs and delayed treatment schedule should reduce the therapeutic effects and survival of patients. Furthermore, there is currently no established prevention or treatment methods for oral mucositis [1-3]. Even if drug were withdrawn, the induced peripheral neuropathy may leave rare recovery and lifelong disability [4-6]. Extravasation is more likely to occur when the peripheral venous wall is fragile or when phlebitis occurs, leading to the constriction and clogging of blood vessels, and then inflammation and necrosis. [7-9].

We have reported previously that many anticancer drugs show strong toxicity to human normal oral epithelial cells [human oral keratinocyte (HOK), human gingival epithelial progenitor cell (HGEP)] and induce apoptosis (loss of microvilli on the cell membrane surface and activation of caspases) in *in vitro* experiments [10]. We have established *in vitro* quantification method of antitumor activity, using four human oral squamous cell carcinoma (OSCC) cell lines (gingival-derived Ca9-22, tongue-derived HSC-2, HSC-3, HSC-4), three human mesenchymal oral normal cells [gingival fibroblast (HGF), periodontal ligament fibroblast (HPLF), and pulp cell (HPC)] and two human epithelial oral normal cells (HOK and HGEP) [11, 12]. Tumor-specificity (TS) was calculated as the ratio of the mean CC₅₀ against normal cells to the mean of CC₅₀ against OSCC cells. When mesenchymal cells (M) or epithelial cells (E) are used, TS_M and TS_E are obtained, respectively. Since most anticancer drugs exhibit strong cytotoxicity against epithelial cells, TS_M values were adopted at the initial stage of comprehensive search for new antitumor substances. Using this method, we found that (i) most anticancer drugs show 1 to 3 orders of magnitude higher tumor-specificity against OSCC cell lines as compared with human oral mesenchymal normal cells yielding the TS_M value of 10-1000, (ii) three major polyphenols, namely lignin glycosides, tannins, and flavonoids, show much lower TS_M value of 1-10, (iii) among 12 series of chromone derivatives and 5 series of esters and amides (a total of 291 compounds), 7-methoxy-3-[(1E)-2-phenylethenyl]-4H-1-benzopyran-4-one (compound A) and 3-[(1E)-2-(4-hydroxyphenyl)ethenyl]-7-methoxy-4H-1-benzopyran-4-one (compound B) showed the greatest tumor selectivity (TS_M=301 and 182, respectively) [13, 14]. However, compounds A and B induced G₂/M phase accumulation [14], suggesting the possible induction of strong neurotoxicity.

We manufacture four or five newly synthesized chromone derivatives every year, expecting to find more active and less adverse compounds than compounds A and B. This time, we newly synthesized a total of 65 compounds: 2-indolylchromones (9 compounds: Series A) [15], indole-auron derivatives (10 compounds: Series B) [16], capsaicin derivatives (23 compounds: Series C) [17, 18], 6,7-styrylchromone derivatives (12 compounds, Series D) [19] and benzyldiene chromanones (11 compounds: Series E) [20] (Figure 1). In the present study, we first investigated whether TS_M values of these newly synthesized compounds exceed those of compounds A and B. Secondly, since this was not the case, further confirming the superiority of the compounds A and B over newly synthesized materials, we investigated the TS_M, TS_E and neurotoxicity of compounds A and B, in comparison with four positive controls, 5-FU, cisplatin (CDDP) and docetaxel (DTX), used clinically for the treatment of OSCC [21], and doxorubicin (DOX). Thirdly, we investigated the possible signaling pathway of compounds A and B, using QSAR prediction based on the Tox21 database.

2. Materials and Methods

2.1. Experimental Materials and Reagents

Dulbecco's modified Eagle's medium (DMEM) was purchased from GIBCO BRL (Grand Island, NY, USA); Fetal bovine serum (FBS), doxorubicin (DOX), 3-(4,5-dimethylthiazol-2-yl)-2,5-diphenyltetrazolium bromide (MTT); Dimethyl sulfoxide (DMSO) and cisplatin (CDDP) from FUJIFILM Wako Chem (Osaka, Japan); 5-fluorouracil (5-FU) from Kyowa (Tokyo, Japan); docetaxel (DTX) from Toronto Research Chemicals (Toronto, Canada); The 100 mm dishes from Trueline (Haryana, India); the 96-hole plates from TPP (Techno Plastic Products AG, Trasadingen, Switzerland).

2.2. Synthesis of Novel Chromone Derivatives

7-Methoxy-3-[(1E)-2-phenylethenyl]-4H-1-benzopyran-4-one (compound A) was synthesized by Knoevenagel condensation of 7-methoxy-3-formylchromone and phenylmalonic acid, as described previously [14,22]. Also, 3-[(1E)-2-(4-hydroxyphenyl)ethenyl]-7-methoxy-4H-1-benzopyran-4-one (compound B) was synthesized by condensation of 7-methoxy-3-formylchromone and 4-(methoxymethoxy)benzeneacetic acid followed by removal the protecting group [22].

2-Indolylchromone 9 compounds (Series A) were synthesized by the conjugated addition reaction of 3-iodochromone derivatives with selected azoles [15]. Indole-auron derivatives 10 compounds (series B) were synthesized by conjugation addition reaction of 3-iodochromone derivatives with the appropriate indoles [16].

Capsaicin derivatives 23 compounds (Series C) were synthesized by the condensation of various fatty acid chlorides with vanillylamine derivatives [17,18].

6,7-Styrylchromone derivatives 12 compounds (series D) were synthesized by the coupling of bromochromones with various styrene derivatives using the Heck reaction [19].

3-Benzylidene chromanone 11 compounds (Series E) were synthesized by base-catalyzed condensation of the appropriate 4-chromanones with substituted benzaldehyde derivatives [20].

2.3. Cells

Human OSCC cell lines Ca9-22 (catalog number: RCB-1976), HSC-2 (RCB-1945), HSC-3 (RCB-1975), HSC-4 (RCB-1902), and a rat cell line derived from malignant peripheral nerve sheath tumor LY-PPB6 (RCB-2729), were purchased from RIKEN Cell Bank (Tsukuba, Ibaraki, Japan). Human oral mesenchymal cells (gingival fibroblast HGF, human periodontal ligament fibroblast HPLF, and human pulp cell HPC) were prepared from the extracted teeth of patients who obtained informed consent [15-20 PDL (population doubling level after primary culture)] with the approval of the internal ethics committee (No. A0808) [23].

The rat pheochromocytoma derived cells PC-12 and human neuroblastoma SH-SY5Y were donated by Dr. Okudaira, Teikyo University School of Medicine. All of these cells were cultured at 37°C, in a humidified 5% CO₂ incubator (MCO-170 AICUVD-P; Panasonic Healthcare Co., Ltd., Gunma, Japan) in DMEM containing 10% heat-inactivated FBS.

Differentiated maturing dPC-12 cells with significantly reduced growth potential, expressing neurites were prepared using an overlay method in which PC-12 cells were layered every 3 days with serum-free DMEM containing 50 ng/mL NGF without discarding the conditioned medium [24].

Gingival epithelial progenitor cells HGEP were purchased from CELLnTEC and cultured in Cnt-PR medium [10].

2.4. Cytotoxicity Assay

After detachment of cells with 0.25% trypsin solution (containing EDTA), 0.1 ml of cell suspension (2×10^4 / ml) was seeded in a 96-microwell plate with triplicate, cultured in a 5% CO₂ incubator at 37°C for 48 h to achieve complete attachment to the plate. After replacement of fresh medium containing samples of various concentrations, cells were further cultured for 48 h to measure the absorbance at 560 nm (that reflect the viable cell number) by MTT method. All samples were dissolved in DMSO. The toxicity of DMSO alone was calculated and subtracted. From the dose-response curve of test samples, 50% cytotoxic concentration (CC₅₀) was determined.

2.5. Tumor-Specificity and Neurotoxicity

Tumor specificity (TS) was calculated as the ratio of the mean of CC₅₀ for normal cells to that for OSCC cells. When mesenchymal cells (M) (HGF, HPLF, HPC) or epithelial cells (E) (HGEP) were used, TS_M and TS_E are obtained, respectively. $TS_M = \text{mean CC}_{50} \text{ against three normal human oral mesenchymal cells (HGF + HPLF + HPC)} / \text{mean CC}_{50} \text{ against four OSCC cell lines (Ca9-22 + HSC-2 + HSC-3 + HSC-4)}$, as shown by D/B in Table 1. Since both Ca9-22 and HGF cells were derived from

gingival tissue, the relative sensitivity of these cells was also compared (as shown by C/A in Table 1). $TSE = CC_{50} (HGEP) / CC_{50} (OSSC)$.

The ratio of mean CC_{50} for undifferentiated neuronal cells (PC-12, SH-SY5Y, LY-PPB6) or differentiated dPC-12 to that for OSCC (defined as TS_N and TS_{DN} , respectively) indicates the safety of neurotoxicity. When the TS_N or TS_{DN} is higher, the ratio of anticancer activity to neurotoxicity is higher. The compounds having the highest TSM , TSE , TS_N and TS_{DN} is the best compound.

2.6. Calculation of Chemical Descriptors

The activities against 59 signaling pathways [25], agonist and antagonist activities of the nuclear receptor, and stress response pathway were calculated by the chemical structures. In other words, all chromone derivatives were classified as positive or negative based on the calculated probabilities in Tox21 activity scores of 1 or higher for each signaling pathway using the Toxicity Predictor, a QSAR based on machine learning models trained on the Tox21 10K compound library [25]. Through Toxicity Predictor, we can wash and standardize the SMILES strings (salt, counterions, fragment removal, and adjustment of protonation state (neutralization)) to determine the optimal 3D conformer. The optimized molecular structures were confirmed using MarvinView (ChemAxon Kft., Budapest, Hungary).

2.7. Statistical Processing

All experiments were conducted in triplicate, and the average value was represented as the mean \pm standard deviations (SD) of triplicate determinations. The significance of values was examined by one-way analysis of variance (ANOVA) and appropriate Bonferroni's post-test. A value of $p < 0.05$ was considered to indicate statistically significant differences.

3. Results

3.1. Continuous Search for New Chromone Derivatives with Higher TSM - Confirmation of Prominent Tumor-Specificity of Compounds A and B

We are continuing to search new chromone derivative having higher TSM than compounds A and B. In the present, we investigated 5 series of chromones derivatives for this purpose (Figure 1) (CC_{50} values described in **Supplementary Data Figure S1**).

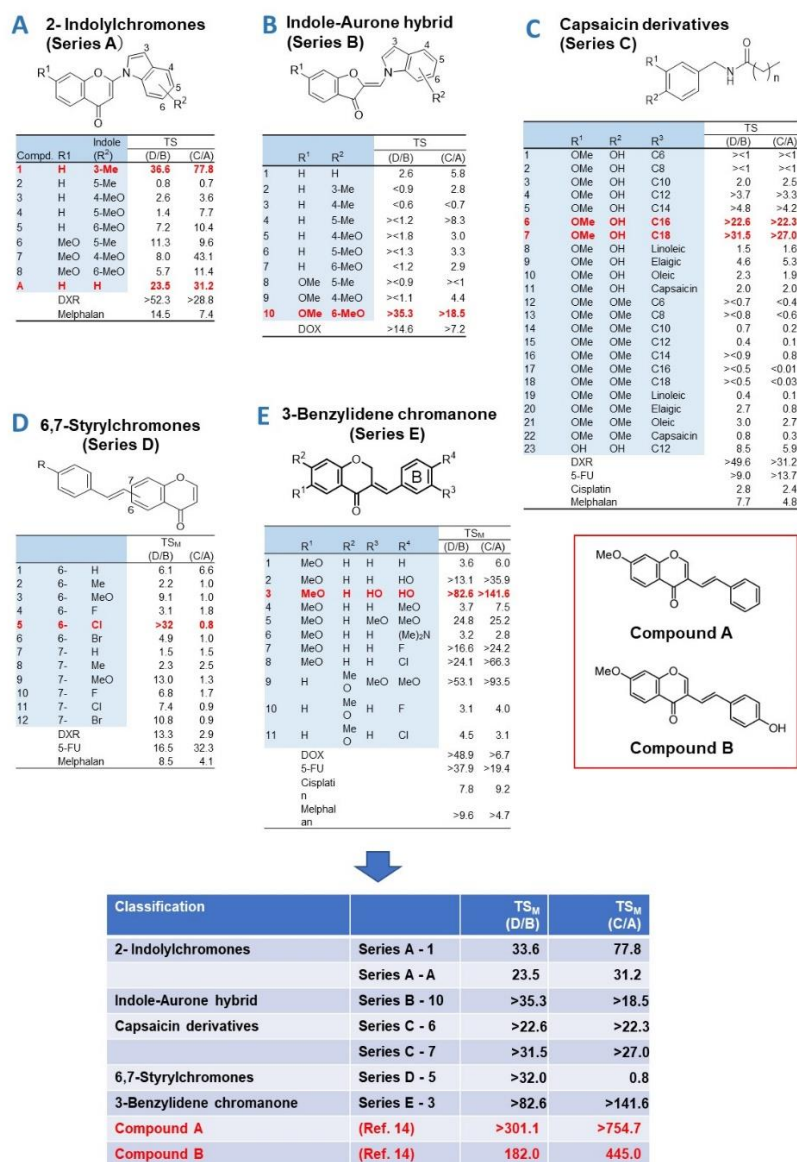


Figure 1. Tumor-specificity of 65 newly synthesized chromone derivatives. (A) 2-Indolylchromones (series A), (B) Capsaicin derivatives (Series C), (C) 6,7-Styrylchromones (Series D), (D) Indole-Aurone hybrid (Series B) and 3-Benzylidene chromanone (Series E).

Among the 2-indolylchromones (9 compounds, Series A), A1 and AA showed the highest TS_M values, 36.6 and 23.5, respectively. When gingival-derived carcinoma Ca9-22 and gingival fibroblast HGF were used as target cells, TS_M values of 77.8 and 31.2 were given, respectively (Figure 1A). Among the indole-aurone hybrids (10 compounds, Series B), B-10 showed the highest TS_M values of >35.3 and >18.5 (Figure 1B).

Among the capsaicin derivatives (23 compounds, Series C), C-6 and C-7 showed the highest TS_M values of >22.6 and >31.5; >22.3 and >27.0 (Figure 1C).

Among the 6,7-styrylchromone derivatives (12 compounds, series D), D5 showed the largest TS_M values of 32.0 and 0.8 (Series 1D).

Among 3-benzylidene chromanones (11 compounds, Series E), E-3 exhibited the highest TS_M value (TS_M=>82.6; >141.6, Figure 1E). The CC₅₀ values for human oral squamous cell lines (Ca9-22, HSC-2, HSC-3, HSC-4) and normal oral cells (HGF, HPLF, HPC) are shown in **Supplemental Material Section (Table S1)**.

These data demonstrated that tumor-specificity of 2-Indolylchromones (A-1, A-A), indole-aurone hybrid (B-10), capsaicin derivatives (C-6, C-7) and 6,7-styrylchromone (D-5) and 3-benzylidene chromanone (E-3) showed some tumor-specificity, but their TS_M values were one order of magnitude

lower than that of compounds A ($TS_M=201.1$, 754.7) and B ($TS_M=182.0$, 445.0) [13, 14]. These results show that compounds A and B showed the highest TS_M values among a total of 356 chromone derivatives so far investigated in our laboratory.

3.2. Rapid Decay of Cell Growth by Chromone Derivatives

Ca9-22 cells were treated with compound A or selected seven compounds for various times, replaced with fresh drug-free medium, and incubated for 48 h after the start of drug administration and then viable cell numbers were then determined by the MTT method (Figure 2). Cytotoxicity of chromone derivatives (series A, C, D, and E compounds) reached the maximum after 24 h-treatment. On the other hand, series B, that belongs to indole-auron derivatives (closed by blue circles) showed rather cytostatic growth inhibition even after 48 h incubation. This suggests that cytotoxic, rather cytostatic growth inhibition, is characteristic to the active chromone derivatives.

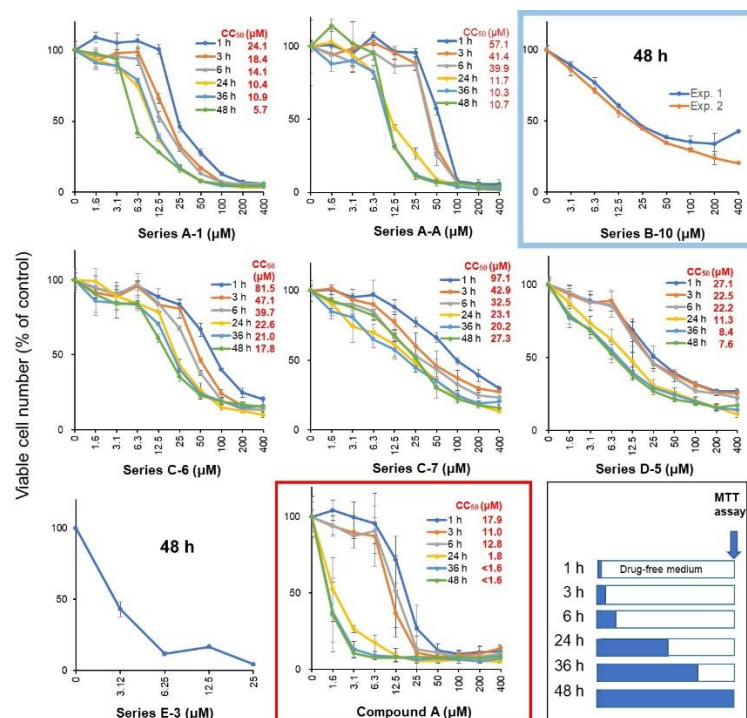


Figure 2. Time course of cytotoxicity induction by chromone derivatives in Ca9-22 cells. Cells were incubated for 1, 3, 6, 24, 36 or 48 h with the indicated concentrations with test samples. After 48 h after adding test samples, cell number was determined by MTT method. Each value represents mean \pm SD of triplicate assays, and expressed as % of control (without sample).

3.3. Higher Tumor-Specificity and Less Neurotoxicity of Compounds A and B than Those of Popular Anticancer Drugs

The 50% cytotoxic concentration (CC_{50}) of compound A to OSCC (Ca9-22, HSC-2) was below 1 μM , as little as 1/400 of CC_{50} for normal oral epithelial system (HGEP) and mesenchymal cells (HGF, HPC). The CC_{50} values for neuronal cells (PC-12, SH-SY5Y, LY-PPB6) were distributed between OSCC and normal oral cells (Figure 3A). Compound B showed similar distribution pattern (Figure 5B). When PC-12 cells were cultured in a medium containing 50 ng/ml NGF in serum-free medium for 2, 5, and 7 days, differentiated dPC-12 cells with elongated neurites gradually increased (Supplementary Figure S1). Differentiated dPC-12 cells with much reducing proliferating activity (closed green) showed similar sensitivity to compounds A and B with undifferentiated PC-12 cells that rapidly grow (open green) (Figure 3AB, closed green). This indicated that higher sensitivity of neuronal cells dose not depend on their growth potential.

5-FU showed cytostatic growth inhibition of cancer cells and epithelial normal cells, without completely killing them (Figure 3C). Cisplatin damaged neuronal cells more potently than against

OSCC cells (Figure 3D). DOX damaged neuronal cells, normal mesenchymal and epithelial cells (Figure 3E). Docetaxel (DTX) at as little as 39 nM showed cytostatic growth inhibition against epithelial normal cells (Figure 3F). In contrast, compounds A and B showed no keratinocyte toxicity up to 400 μ M (Figure 3A and B).

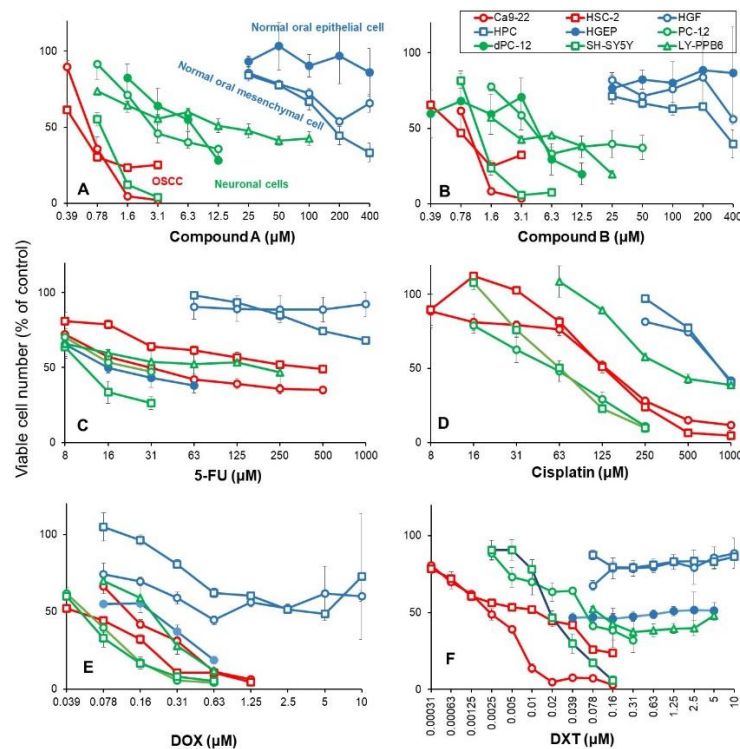


Figure 3. Compounds A/B induced higher cytotoxic activity against OSCC cell lines, and milder neurotoxicity than 5-FU, cisplatin and doxorubicin. Cells were incubated for 48 h with the indicated concentrations of test samples. After 48 h, cell number was determined by MTT method. Each value represents mean \pm SD of triplicate assays and expressed as % of control (without sample).

Based on these results, the tumor-specificity and neurotoxicity of compound A, compound B, and four typical anticancer drugs were quantified (Table 1). When the mean CC_{50} values for OSCC (Ca9-22, HSC-2), human normal mesenchymal cells (HGF, HPLF), gingival epithelial progenitor HGP neuronal cells (PC-12, SH-SY5Y, LY-PPB6), and differentiated dPC-12 were defined as A, B, C, D, and E, the tumor-specificity for OSCC can be calculated by the following equation: $TS_M = B / A$ (compared to mesenchymal normal oral cells), $TS_E = C / A$ (compared to epithelial normal oral cells), $TS_N = D / A$ (compared to neuronal cells), and TS_{DN} (compared to differentiated PC-12 cells). Compounds A and B showed high selective toxicity to OSCC, regardless of using either mesenchymal cells ($B/A = 475.6, 429.9$) or epithelial cells ($C/A = 661.8, 497.4$) as normal cells. On the other hand, DTX showed the maximum TS_M value ($B/A = 1316.9$), but much reduced TS_E value when epithelial cells were used ($C/A = 5.1$). DOX showed 6 times lower TS_M value than compound A ($B/A = 75.9$), and very low TS_E ($C/A = 2.3$). 5-FU and cisplatin showed low selective toxicity to OSCC in both mesenchymal and epithelial cells ($B/A=4.52, 6.5, C/A=0.07$).

All six drugs used in this study showed strong neurotoxicity. Among these, compound A ($D / A = 11.1$) showed the weakest neurotoxicity, followed by DTX ($D / A = 7.9$) and compound B ($D / A = 3.1$). DOX, cisplatin, and 5-FU were found to damage neuronal cells at the concentrations that damage OSCC ($D/A=1.2, 1.3, 0.3$) (Table 1).

Table 1. Higher tumor-specificity and lesser neurotoxicity of compounds A and B than those of popular anti-cancer drugs.

		CC ₅₀ (μM)					
		Compound A	Compound B	5-FU	Cisplatin	DOX	DTX
Human oral squamous cell carcinoma cells							
Ca9-22		0.68	0.95	31.0	137.4	0.13	0.002
HSC-2		0.53	0.72	411.3	130.1	0.05	0.013
mean	(A)	0.60	0.83	221.1	133.7	0.09	0.008
Human normal oral mesenchymal cells							
HGF		>400	>400	>1000	876.1	>10	>10
HPC		174.9	317.3	>1000	871.3	3.7	>10
mean	(B)	>287.4	>358.6	>1000	873.7	>6.8	>10
Human normal oral epithelial cells							
HGEP	(C)	>400	>400	15.5	N.D. ¹	0.21	0.039
Undifferentiated neuronal cells							
PC-12		2.9	4.2	24.0	58.2	0.060	0.063
SH-SY5Y		0.9	1.2	11.3	63.7	0.053	0.019
LY-PPB6		16.3	2.4	190.4	381.0	0.21	0.10
mean	(D)	6.7	2.6	75.2	167.6	0.11	0.060
Differentiated PC12 cells							
dPC-12	(E)	7.5	4.7				
Tumor-specificity							
TS _M	(B/A)	>475.6	>429.9	>4.5	6.5	>75.9	>1316.9
TS _E	(C/A)	>661.8	>479.4	0.070	N.D.	2.3	5.1
TS _N	(D/A)	11.1	3.1	0.34	1.3	1.2	7.9
TS _{D_N}	(E/A)	12.4	5.6				

¹ N.D., not determined.

4. Discussion

4.1. Rational of Using Human Normal Oral Cells as a First Stage of Screening of High TS_M Cells

Since many anticancer drugs are known to induce oral mucosal diseases and neurotoxicity, it is important to manufacture the compounds having higher tumor-specificity and lower adverse effects. In addition, considering future clinical applications, it is desirable to use human-derived cancer cells and normal cells as target cells. In this study, anticancer drugs (DTX, cisplatin, 5-FU, DOX) used as positive controls, showed high cytotoxicity against normal epithelial cells (Table 1), therefore we used human oral squamous cells (OSCCs) and human mesenchymal oral normal cells to quantify tumor selectivity at the initial screening stage.

4.2. Failure of 65 Newly Synthesized Chromones Derivatives to Exceed the TS_M of Chromones A and B

Previous studies have reported that among 291 chromone derivatives, compounds A and B showed the greatest tumor selectivity [13, 14]. In this study, we challenged to investigate a total of 65 new compounds (classified into 5 groups), hoping we may find more potent antitumor substances. Contrary to our expectation, TS_M of any of these compounds did not exceed that of compounds A and B (Figure 1). This shows that compounds A and B are the most potent chromone derivatives so far investigated. Based on these results, the side effects of compounds A and B and four anticancer drugs were next compared at the same time.

4.3. Comparison of Antitumor Potential and Adverse Effects of Chromones A and B with Four Popular Anticancer Drugs

4.3.1. Tumor-Specificity

DTX showed the greatest tumor selectivity ($TS_M=1316.9$), followed by compound A (475.6) > compound B (429.9), DOX (75.9) >> cisplatin (6.5) > 5-FU (4.5), confirming our previous findings [10, 13, 14, 26]. Since 5-FU showed only cytostatic growth inhibition rather than cytotoxic action (Figure 5C), concomitant use of other anticancer drugs may be a good choice. Actually, 5-FU combined with oxaliplatin significantly increased survival of cancer patients [27].

4.3.2. Keratinocyte Toxicity

When tumor-specificity was evaluated with OSCC and human normal epithelial cell lines, TS_E values of compounds A and B (661.8 and 479.4, respectively) were approximately two-fold higher than those of DTX and DOX (5.1 and 2.3, respectively) (Table 1). We also reported previously that (*E*)-3-(4-hydroxystyryl)-6-methoxy-4*H*-chromen-4-one showed one to two-fold higher TS_E values than DOX and 5-FU, and induced the mitochondrial vacuolization, autophagy suppression followed by apoptosis induction, and changes in the metabolites involved in amino acid and glycerophospholipid metabolisms [28].

4.3.3. Neurotoxicity

We next investigated the ratio of OSCC toxicity / neurotoxicity (equivalent to TS_N). Compound A showed the highest TS_N value ($TS_N=11.1$, $TS_{ND}=12.4$), followed by DTX (7.9) > compound B ($TS_N=3.1$, $TS_{ND}=5.6$) > cisplatin ($TS_N=1.3$) > DOX ($TS_N=1.2$) > 5-FU ($TS_N=0.3$). These data suggests that compounds A and B, and DTX shows higher cytotoxicity against OSCC than neuronal cells. On the other hand, DOX, cisplatin, and 5-FU damaged both OSCC and neurons to comparable extent. Paclitaxel-induced neurotoxicity has been reported to be suppressed by the addition of antioxidants (such as docosahexaenoic acid, acetyl-L-carnitine hydrochloride, *N*-acetyl-L-cysteine and sodium ascorbate) in cultured cells [29]. Also, in animal studies in rats, DOX-induced neurotoxicity and behavioral was potentially protected by coenzyme Q10 [30], and DOX-induced cardiotoxicity is significantly suppressed with candesartan and quercetin [31]. For Compound A, we plan to search for drugs that alleviate the neurotoxicity and enhance the toxicity to OSCC.

4.4. Search for Target Molecules

Both compound A and docetaxel accumulated Ca9-22 cells in the G₂/M phase, but the former has a cytocidal action, while the latter exhibits a cytostatic effect (Figure 5A, F), confirming previous report with compound A [14] and docetaxel [25, 27], suggesting different site of action. The possibility of microtubule inhibition in neurotoxicity should also be investigated [32,33].

At present, the target site of compounds A and B is not identified. Nuclear receptors and stress response pathways that are possibly involved in the inhibition of OSCC growth by compounds A and B were searched using Toxicity Predictor [23]. The specific cytotoxicity of 14 chromone derivatives including compounds A and B against OSCC cells were correlated with estrogen-related receptor inhibitory activity (ERRPGC_ant) in the presence of PPAR γ activators (Figure 4), but not with other 58 signaling pathways (Table 2). These data suggest that compounds A and B may inhibit the signaling pathway of estrogen-related receptors.

We recently reported that compound B potently inhibited the HMGB1-stimulated IL-6 production in mouse macrophage-like cells RAW264.7, suggesting dual suppressive actions: anti-inflammatory and anticancer activities [34]. Compound B (10 μ M) failed to inhibit the following kinases (ABL, CSK, EDRF, EPHA2, EPHB4, FGFR1, FLT3, IGF1R, ITK, JAK3, KDR, LCK, MET, PDGFR α , PYK2, SRC, SYK, TIE2, TRKA, TYRO3)(unpublished data). If the target site is known, it will lead to create more selective materials.

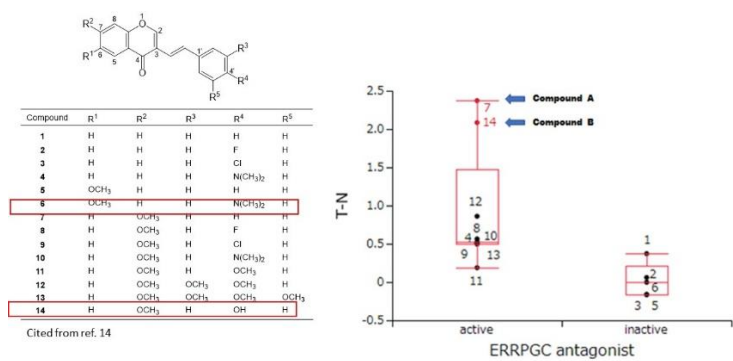


Figure 4. Prediction of Estrogen related receptor with PPAR γ coactivator antagonist activities (ERRPGC_ant) of compounds A and B by Toxicity Predictor. In silico study suggests the inhibition of compound A against the estrogen related receptor-alpha signaling pathway, that is identified as an adverse marker for breast cancer progression and poor prognosis. Data of CC₅₀ and TSM values were derived from previous study (15). Tumor selectivity is defined by the balance between pCC₅₀ values for normal (N) and tumor (T) cells. The difference (T-N) was used as a tumor-selectivity index only for this analyse. When pCC₅₀ is defined as -log (CC₅₀), T-S can be calculated as: pCC₅₀ (T) – pCC₅₀ (N) = log CC₅₀ (N)- log CC₅₀ (T) = log (CC₅₀(N)-log (CC₅₀(T)) =log CC₅₀ (N/T).

Table 2. Search for possible signaling pathway of compounds A/B-induced tumor-specific cytotoxicity.

Signaling pathway investigated	p-value
ERRPGC_ant (estrogen related receptor with PGC antagonist)	0.0307 ¹
CAR_ant (constitutive androstane receptor antagonist)	0.1385
RAR_ant (retinoic acid receptor antagonist)	0.1472
ARant_ago (androgen receptor with antagonist agonist)	0.1567
TSHR_ago (thyroid stimulating hormone receptor agonist)	0.1619
H2AX_ago (histone variant H2AX agonist)	0.1825
GR_ant (glucocorticoid receptor antagonist)	0.2328
TRHR_ago (thyrotropin releasing hormone receptor agonist)	0.2913
TR_ant (thyroid receptor antagonist)	0.3295
PPARg_ant (peroxisome proliferator-activated receptor gamma antagonist)	0.3348
CaspC_ind (caspase-3/7 in CHO-K1 inducer)	0.3508
HDAC_ant (histone deacetylase antagonist)	0.3539
TRHR_ant (thyrotropin releasing hormone receptor antagonist)	0.3812
ERb_ant (estrogen receptor beta antagonist)	0.4774
RXR_ago (retinoid X receptor-alpha agonist)	0.4933
FXR_ago (farnesoid-X-receptor agonist)	0.5155
TSHR_ant (thyroid stimulating hormone receptor antagonist)	0.5234
ERRPGC_ago (estrogen related receptor with PGC agonist)	0.5461
TGFb_ant (transforming growth factor beta antagonist)	0.5573
CaspH_ind (caspase-3/7 in HepG2 inducer)	0.5673
ERlbd_ago (estrogen receptor alpha lbd agonist)	0.6411
ROR_ant (retinoid-related orphan receptor gamma antagonist)	0.6582
PPARd_ant (peroxisome proliferator-activated receptor delta antagonist)	0.6642
PR_ant (progesterone receptor antagonist)	0.724
ERsr_ago (endoplasmic reticulum stress response agonist)	0.8102
ARlbd_ant (androgen receptor lbd antagonist)	0.8227
ERR_ago (estrogen related receptor agonist)	0.8391
MMP_disr (mitochondrial membrane potential disruptor)	0.8582
ARfull_ant (androgen receptor full antagonist)	0.8582

ARfull_ant (androgen receptor full antagonist)	1.8582
ARfull_ant (androgen receptor full antagonist)	2.8582
ARfull_ant (androgen receptor full antagonist)	3.8582
ARfull_ant (androgen receptor full antagonist)	4.8582
ARfull_ant (androgen receptor full antagonist)	5.8582
ARfull_ant (androgen receptor full antagonist)	6.8582
ARfull_ant (androgen receptor full antagonist)	7.8582
ARfull_ant (androgen receptor full antagonist)	8.8582
ARfull_ant (androgen receptor full antagonist)	9.8582
ARfull_ant (androgen receptor full antagonist)	10.8582
ARfull_ant (androgen receptor full antagonist)	11.8582
ARfull_ant (androgen receptor full antagonist)	12.8582
ARfull_ant (androgen receptor full antagonist)	13.8582
ARfull_ant (androgen receptor full antagonist)	14.8582
ARfull_ant (androgen receptor full antagonist)	15.8582
ARfull_ant (androgen receptor full antagonist)	16.8582
ARfull_ant (androgen receptor full antagonist)	17.8582
ARfull_ant (androgen receptor full antagonist)	18.8582
ARfull_ant (androgen receptor full antagonist)	19.8582
ARfull_ant (androgen receptor full antagonist)	20.8582
ARfull_ant (androgen receptor full antagonist)	21.8582
ARfull_ant (androgen receptor full antagonist)	22.8582
ARfull_ant (androgen receptor full antagonist)	23.8582
ARfull_ant (androgen receptor full antagonist)	24.8582
ARfull_ant (androgen receptor full antagonist)	25.8582
ARfull_ant (androgen receptor full antagonist)	26.8582
ARfull_ant (androgen receptor full antagonist)	27.8582
ARfull_ant (androgen receptor full antagonist)	28.8582
ARfull_ant (androgen receptor full antagonist)	29.8582
ARfull_ant (androgen receptor full antagonist)	30.8582

¹ Detailed QSAR analysis and calculations are shown in **Supplementary Materials: Table S2**.

There was a possibility that higher drug sensitivity of neuronal cells may be due to their high proliferative capacity. However, this possibility seems to be low, since both undifferentiated PC-12 cells (rapidly growing) and differentiated PC-12 cells (growth retarded) [24] showed comparable sensitivity to compounds A and B (Figure 3A and B). Experiments using primary neurons that have stopped dividing and maintained their nerve function may support this point.

5. Conclusions

Chromone ring is widely distributed into flavonoids such as flavonol, flavone, flavanone and isoflavone. Compound A has with a styryl series attached to chromone ring (Figure 2) derived from natural products and therefore can be easily adaptable to living organisms. Compound A has higher tumor selectivity against OSCC cells than the low-molecular polyphenols and anticancer drugs 5-FU, cisplatin, and DOX, which many researchers have worked on, and has weaker keratinocyte toxicity and neurotoxicity. It is thus expected to be a potential lead compound for the discovery of new oral cancer therapeutic drugs.

Supplementary Materials: The following supporting information can be downloaded at the website of this paper posted on Preprints.org., **Figure S1:** Induction of neurite extension in PC-12 cells by NGF, **Table S1:** Tumor-specificity of newly synthesized 65 chromone derivatives, **Table S2:** Search for signaling pathway involved in 3-styrylchromone induced-induced selective tumor-specificity against human OSCC cell lines.

Author Contributions: Conceptualization, H.S. and Y.U.; methodology, H.S.; software, Y.U.; investigation, T.A., H.S., S.A., S.U., K.B. and A.S.; resources, S.U., H.Sh, Y.T., Y.K., K.T. and Y.S.; writing—original draft preparation, H.S.; writing—review and editing, H.S., S.T.; supervision, H.T.; funding acquisition, H.S. All Authors read and approved the final version of the article.

Funding: This research was partially carried out by the Grants-in-Aid for Scientific Research of the Japan Society for the Promotion of Japan ((1) Grant-in-Aid for Scientific Research (C) 20K09885: Elucidation of the selective toxicity mechanism of chromone derivatives for cancer cells, Principal Investigator: Hiroshi Sakagami; (2) Grant-in-Aid for Scientific Research (C) 16K11519: Basic research on the potential of a novel 3-styrylchromone derivative as a therapeutic agent for oral cancer, Principal Investigator Hiroshi Sakagami).

Institutional Review Board Statement: Ethical review and approval were waived for this study since we used only cultured cells that had been purchased from the RIKEN Cell Bank and the human normal oral cells established in our laboratory 11 years ago according to the guidelines of the intramural Ethics Committee (No. A0808).

Informed Consent Statement: Not applicable since we used only cultured cells.

Acknowledgments: The authors would like to express deepest gratitude to Prof. Tamura, Dr. M. Kobayashi, and Dr. R. Matsuda, Meikai University School of Dentistry, for their secretary work.

Conflicts of Interest: The authors declare no conflict of interest.

References

1. Elad, S.; Yarom, N.; Zadik, Y.; Kuten-Shorrer, M.; Sonis, S. T., The broadening scope of oral mucositis and oral ulcerative mucosal toxicities of anticancer therapies. *CA Cancer J Clin* **2022**, *72* (1), 57-77.
2. Murdock, J. L.; Reeves, D. J., Chemotherapy-induced oral mucositis management: A retrospective analysis of MuGard, Caphosol, and standard supportive care measures. *J Oncol Pharm Pract* **2020**, *26* (3), 521-528.
3. Tanaka, Y.; Ueno, T.; Yoshida, N.; Akutsu, Y.; Takeuchi, H.; Baba, H.; Matsubara, H.; Kitagawa, Y.; Yoshida, K., Is Oral Mucositis Occurring During Chemotherapy for Esophageal Cancer Patients Correctly Judged? EPOC Observational Cohort Study. *Anticancer Res* **2019**, *39* (8), 4441-4448.
4. Brinkmann, V.; Fritz, G., Prevention of anticancer therapy-induced neurotoxicity: Putting DNA damage in perspective. *Neurotoxicology* **2022**, *91*, 1-10. doi: 10.1016/j.neuro.2022.04.009
5. Li, T.; Mizrahi, D.; Goldstein, D.; Kiernan, M. C.; Park, S. B., Chemotherapy and peripheral neuropathy. *Neurol Sci* **2021**, *42* (10), 4109-4121.
6. Fumagalli, G.; Monza, L.; Cavaletti, G.; Rigolio, R.; Meregalli, C., Neuroinflammatory Process Involved in Different Preclinical Models of Chemotherapy-Induced Peripheral Neuropathy. *Front Immunol* **2020**, *11*, 626687. doi: 10.3389/fimmu.2020.626687
7. Ehmke N. Chemotherapy Extravasation: Incidence of and Factors Associated With Events in a Community Cancer Center. *Clin J Oncol Nurs* **25**(6), 680-686, 2021. doi: 10.1188/21
8. Boulanger, J.; Ducharme, A.; Dufour, A.; Fortier, S.; Almanric, K., Management of the extravasation of anti-neoplastic agents. *Support Care Cancer* **2015**, *23* (5), 1459-71.
9. Bahrami, M.; Karimi, T.; Yadegarfar, G.; Norouzi, A., Assessing the Quality of Existing Clinical Practice Guidelines for Chemotherapy Drug Extravasation by Appraisal of Guidelines for Research and Evaluation II. *Iran J Nurs Midwifery Res* **2019**, *24* (6), 410-416.
10. Sakagami, H.; Okudaira, N.; Masuda, Y.; Amano, O.; Yokose, S.; Kanda, Y.; Suguro, M.; Natori, T.; Oizumi, H.; Oizumi, T., Induction of Apoptosis in Human Oral Keratinocyte by Doxorubicin. *Anticancer Res* **2017**, *37* (3), 1023-1029.
11. Sakagami, H.; Chowdhury, S.A.; Suzuki, F.; Hashimoto, K.; Hatano, H.; Takekawa, H.; Ishihara, M.; Kikuchi, H.; Nishikawa, H.; Taniguchi, S.; Ito, H.; Hatano, T.; Yoshida, T.; Fukai, T.; Shirataki, Y.; Kawase, M.; Watanabe, K.; Mimaki, Y.; Itoh, K.; Horiuchi, A.; Chai, W.; Horiuchi, A.; Motohashi, N., Tumor-specific cytotoxic activity of polyphenols, terpenoids, ketones and other synthetic compounds. Functional Polyphenols and Carotenoids with Antioxidative Action, ed., Motohashi, Research Signpost, Kerala, India, pp133-176, May, 2005.
12. Sakagami, H., Biological activities and possible dental application of three major groups of polyphenols. *J Pharmacol Sci* **2014**, *126* (2), 92-106.

13. Sugita, Y.; Takao, K.; Uesawa, Y.; Nagai, J.; Iijima, Y.; Sano, M.; Sakagami, H., Development of Newly Synthesized Chromone Derivatives with High Tumor Specificity against Human Oral Squamous Cell Carcinoma. *Medicines (Basel)* **2020**, *7* (9). doi: 10.3390/medicines7090050
14. Takao, K.; Hoshi, K.; Sakagami, H.; Shi, H.; Bandow, K.; Nagai, J.; Uesawa, Y.; Tomomura, A.; Tomomura, M.; Sugita, Y., Further Quantitative Structure-Cytotoxicity Relationship Analysis of 3-Styrylchromones. *Anticancer Res* **2020**, *40* (1), 87-95.
15. Sakagami H, Okudaira N, Uesawa Y, Takao K, Kagaya H and Sugita Y: Quantitative Structure-Cytotoxicity Relationship of 2-Azolychromones. *Anticancer Res* 38(2): 763-770, 2018. doi: 10.21873/anticancer.12282. PMID: 29374700
16. Takao, K.; Noguchi, K.; Hashimoto, Y.; Shirahata, A.; Sugita, Y., Synthesis and evaluation of fatty acid amides on the N-oleylethanolamide-like activation of peroxisome proliferator activated receptor α . *Chem Pharm Bull (Tokyo)* **2015**, *63* (4), 278-85. doi: 10.1016/j.bioorg.2019.03.042. PMID: 30933784
17. Takao, K.; U, S.; Kamauchi, H.; Sugita, Y., Design, synthesis and evaluation of 2-(indolylmethylidene)-2,3-dihydro-1-benzofuran-3-one and 2-(indolyl)-4H-chromen-4-one derivatives as novel monoamine oxidases inhibitors. *Bioorg Chem* **2019**, *87*, 594-600.
18. Sakagami, H.; Uesawa, Y.; Ishihara, M.; Kagaya, H.; Kanamoto, T.; Terakubo, S.; Nakashima, H.; Takao, K.; Sugita, Y., Quantitative Structure-Cytotoxicity Relationship of Oleoylamides. *Anticancer Res* **2015**, *35* (10), 5341-51. PMID: 26408695
19. Patonay T, Vasas A, Kiss-Szikszai A, Silva AMS and Cavaleiro JAS. Efficient Synthesis of Chromones with Alkenyl Functionalities by the Heck Reaction. *Aust J Chem* 63: 1582–1593, 2010 DOI: 10.1071/CH10295
20. Uesawa, Y.; Sakagami, H.; Kagaya, H.; Yamashita, M.; Takao, K.; Sugita, Y., Quantitative Structure-cytotoxicity Relationship of 3-Benzylidenechromones. *Anticancer Res* 2016, *36* (11), 5803-5812. doi: 10.21873/anticancer.11164. PMID: 27793902
21. Fu, J. Y.; Yue, X. H.; Dong, M. J.; Li, J.; Zhang, C. P., Assessment of neoadjuvant chemotherapy with docetaxel, cisplatin, and fluorouracil in patients with oral cavity cancer. *Cancer Med* **2023**, *12* (3), 2417-2426. doi: 10.1002/cam4.5075.
22. Takao, K.; Takemura, Y.; Nagai, J.; Kamauchi, H.; Hoshi, K.; Mabashi, R.; Uesawa, Y.; Sugita, Y., Synthesis and biological evaluation of 3-styrylchromone derivatives as selective monoamine oxidase B inhibitors. *Bioorg Med Chem* **2021**, *42*, 116255
23. Kantoh, K.; Ono, M.; Nakamura, Y.; Nakamura, Y.; Hashimoto, K.; Sakagami, H.; Wakabayashi, H., Hormetic and anti-radiation effects of tropolone-related compounds. *In Vivo* **2010**, *24* (6), 843-51.
24. Sakagami, H.; Shi, H.; Bandow, K.; Tomomura, M.; Tomomura, A.; Horiuchi, M.; Fujisawa, T.; Oizumi, T., Search of Neuroprotective Polyphenols Using the "Overlay" Isolation Method. *Molecules* **2018**, *23* (8). doi:10.3390/molecules23081840
25. Kurosaki, K.; Wu, R.; Uesawa, Y., A Toxicity Prediction Tool for Potential Agonist/Antagonist Activities in Molecular Initiating Events Based on Chemical Structures. *Int J Mol Sci* **2020**, *21* (21). doi: 10.3390/ijms21217853. PMID: 33113912.
26. Iijima, Y.; Bandow, K.; Sano, M.; Hino, S.; Kaneko, T.; Horie, N.; Sakagami, H., In Vitro Assessment of Antitumor Potential and Combination Effect of Classical and Molecular-targeted Anticancer Drugs. *Anticancer Res* **2019**, *39* (12), 6673-6684. doi: 10.21873/anticancer.13882. PMID: 31810932
27. Song, J. H.; Lee, J. H.; Kim, S. H.; Um, J. W., Oxaliplatin-based adjuvant chemotherapy rather than fluorouracil-based chemotherapy in rectal cancer is more efficient to decrease distant metastasis and increase survival after preoperative chemoradiotherapy and surgery: a meta-analysis. *Int J Colorectal Dis* **2022**, *37* (3), 649-656. doi: 10.1007/s00384-022-04096-9. PMID: 35050402
28. Sakagami, H.; Shimada, C.; Kanda, Y.; Amano, O.; Sugimoto, M.; Ota, S.; Soga, T.; Tomita, M.; Sato, A.; Tanuma, S.-I.; Takao, K.; Sugita, Y. Effects of 3-styrylchromones on metabolic profiles and cell death in oral squamous cell carcinoma cells. *Toxicol Rep* **2015**, *2*, 1281-1290. doi: 10.1016/j.toxrep.2015.09.009. PMID: 28962471
29. Hara, Y.; Sakagami, H.; Shi, H.; Abe, T.; Tamura, N.; Takeshima, H.; Horie, N.; Kaneko, T.; Shiratsuchi, H.; Kaneko, T., Partial Protection of Paclitaxel-induced Neurotoxicity by Antioxidants. *In Vivo* **2018**, *32* (4), 745-752.
30. Okudan, N.; Belviranlı, M.; Sezer, T., Potential Protective Effect of Coenzyme Q10 on Doxorubicin-Induced Neurotoxicity and Behavioral Disturbances in Rats. *Neurochem Res* **2022**, *47* (5), 1280-1289. doi: 10.1007/s11064-021-03522-8. Epub 2022 Jan 3. PMID: 34978671
31. Majhi, S.; Singh, L.; Yasir, M., Evaluation of Ameliorative Effect of Quercetin and Candesartan in Doxorubicin-Induced Cardiotoxicity. *Vasc Health Risk Manag* **2022**, *18*, 857-866. doi: 10.2147/VHRM.S381485. PMID: 36536768
32. Hou, Y.; Zhao, C.; Xu, B.; Huang, Y.; Liu, C., Effect of docetaxel on mechanical properties of ovarian cancer cells. *Exp Cell Res* **2021**, *408* (1), 112853. doi: 10.1016/j.yexcr.2021.112853

33. Yu, B.; Liu, Y.; Luo, H.; Fu, J.; Li, Y.; Shao, C., Androgen receptor splicing variant 7 (ARV7) inhibits docetaxel sensitivity by inactivating the spindle assembly checkpoint. *J Biol Chem* **2021**, 296, 100276. doi: 10.1016/j.jbc.2021.100276
34. Tanuma, S. I.; Oyama, T.; Okazawa, M.; Yamazaki, H.; Takao, K.; Sugita, Y.; Amano, S.; Abe, T.; Sakagami, H., A Dual Anti-Inflammatory and Anti-Proliferative 3-Styrylchromone Derivative Synergistically Enhances the Anti-Cancer Effects of DNA-Damaging Agents on Colon Cancer Cells by Targeting HMGB1-RAGE-ERK1/2 Signaling. *Int J Mol Sci* **2022**, 23 (7) doi: 10.3390/ijms23073426.

Disclaimer/Publisher's Note: The statements, opinions and data contained in all publications are solely those of the individual author(s) and contributor(s) and not of MDPI and/or the editor(s). MDPI and/or the editor(s) disclaim responsibility for any injury to people or property resulting from any ideas, methods, instructions or products referred to in the content.